

Identification of a strong emission line at $2.8935\mu\text{m}$ in the spectrum of the Orion Nebula

L. B. Lucy

Astrophysics Group, Blackett Laboratory, Imperial College of Science, Technology and Medicine, Prince Consort Road, London SW7 2BW
E-mail: l.lucy@ic.ac.uk

6 December 2018

ABSTRACT

A strong emission line at $2.8935\mu\text{m}$ discovered by Rubin et al. (2001) in an ISO SWS02 spectrum of the Orion Nebula is identified as the $4p\ ^3P - 4s\ ^3S^o$ multiplet of O I. Line formation is due to de-excitation cascades following UV-pumping of high $^3S^o$ and $^3D^o$ terms and occurs in the O I zone immediately behind the Hydrogen ionization front. This cascade mechanism also accounts for permitted O I triplet lines in the Nebula's optical spectrum (Grandi 1975). An escape probability treatment of the O I cascades accounts for the strength of the $\lambda 2.89\mu\text{m}$ line and suggests interesting diagnostic possibilities for the optical lines.

Key words: ISM: Orion Nebula - Line: formation

1 INTRODUCTION

Rubin et al. (2001) have recently reported the detection of an unidentified (uid) strong emission line in an ISO SWS02 spectrum of the Orion Nebula. They also report indications of the line's presence on two spectra from the ISO archive taken at other locations in the Nebula and strong confirmation of the line's reality in a UKIRT long-slit spectrum at the first location. Assuming the line arises in the main ionization zone, they determine the line's vacuum wavelength to be $2.89350\mu\text{m}$.

Unidentified weak lines in astronomical spectra are of course common. But this line is strong, being a factor of only 3.6 weaker than the nearby H I 11-5 line at $\lambda 2.87\mu\text{m}$. Given the efforts of many astronomers since the 1930's in studying the formation of emission lines in photoionized nebulae, either as diagnostics or as coolants, the discovery of a strong uid line at this late date is surprising and potentially of major significance.

Rubin et al. (2001) report their own attempts to identify this line. They note satisfactory wavelength agreement for forbidden lines from two ionic species: Cr III and Fe V, but argue against either being the correct identification. In this paper, an independent effort to identify this line is reported, which was started after seeing their IAU Abstract (Rubin et al. 2000). The search for candidates was based on the Kurucz-Bell (1995) compilation of lines and gf -values.

2 REQUIRED EMISSIVITY

If, following Rubin et al (2001), we assume that the uid line originates in the main ionization zone, then its emissivity can

be estimated from its strength relative to that of the nearby H line. Adopting $T_e = 9000\text{K}$ and $N_e = 4000\text{cm}^{-3}$ as typical for the Orion H II region (Osterbrock, Tran & Veilleux 1992) and setting $N(H^+) = N_e$, we find from Storey & Hummer (1995) that the Case B recombination emissivity of the 11-5 H I line at $\lambda 2.87\mu$ is $8.8 \times 10^{-21}\text{erg s}^{-1}\text{cm}^{-3}$. Accordingly, if the unknown emitting species has the same distribution as H^+ , the uid line's emissivity is

$$4\pi j_{2.89\mu} \simeq 2.4 \times 10^{-21}\text{erg s}^{-1}\text{cm}^{-3} \quad (1)$$

Any proposed identification for which the emission originates within the H II region must be capable of emitting at this rate.

3 REJECTED CANDIDATES

In this section, candidates found on the basis of wavelength coincidence are reported and reasons given for their rejection. Because this work partly duplicates that of Rubin et al. (2001), the discussion is abbreviated.

An excellent candidate on the basis of wavelength is a forbidden line of Chromium at $2.89349\mu\text{m}$. This was discarded immediately because of the low cosmic abundance of this element. Rubin et al. were more persistent but eventually also concluded against this identification, with the stronger argument that three other [Cr III] lines in the IR are not seen in their spectra.

Another similarly acceptable candidate is a forbidden line of Fe V at $\lambda 2.89343\mu\text{m}$. Rubin et al. reject this candidate since the ionization potential of Fe IV (54.8eV) slightly exceeds that of He II (54.4eV), implying a negligible rate of

creation of Fe v ions by photoionization. But, given that Rubin et al. (2000) had evidently failed to find an identification from among the ions expected to be abundant in the H II region, the Fe v possibility was pursued further.

Statistical equilibrium calculations to predict emissivities for the rich spectrum of [Fe v] lines were carried out using the A-values of Garstang (1957) and the collision strengths of Berrington (2001). For $T_e = 9000\text{K}$ and $N_e = 4000\text{cm}^{-3}$, the emissivity per Fe v ion of the transition $3d^4\ ^3G_5 - 3d^4\ ^3F_2$ at $\lambda 2.89343\mu\text{m}$ is $0.93 \times 10^{-20}\ \text{ergs}^{-1}\ \text{cm}^{-3}$. Accordingly, to achieve the target emissivity given in equation (1), the number density of Fe v ions must be $\simeq 0.26\text{cm}^{-3}$. But at $N_e = 4000\text{cm}^{-3}$ and with an Fe abundance $n(\text{Fe})/n(\text{H}) = -4.49\text{dex}$ (Seaton et al. 1994), the number density of Fe atoms is only $\simeq 0.13\text{cm}^{-3}$. If further evidence against this identification were needed, these calculations reveal that there are several other [Fe v] lines in the IR with greater emissivities, including two from the same upper level as this rejected candidate.

4 PROPOSED CANDIDATE

The suggested identification is the O I multiplet $4p\ ^3P - 4s\ ^3S^o$. The permitted components of this multiplet are at vacuum wavelengths 2.89330, 2.89352 and $2.89359\mu\text{m}$ with gf-values of 0.50, 2.51 and 1.50, respectively.

Two mechanisms of line formation will be considered in this section in an attempt to justify this identification. The aim is to demonstrate that emission in this transition can plausibly account for the maximum observed line brightness. No attempt is made to give a definitive treatment of line formation.

4.1 Atomic data

The atomic model is restricted to the O I triplet system. Specifically, all terms in the $^3S^o$, 3P , $^3D^o$ and 3F series are included up to principal quantum numbers $n = 11, 10, 11$ and 10, respectively. Energy levels are the experimental values from the NIST Atomic Spectra Database if available. For higher n , we take

$$E_n = E_\infty - \frac{R_O}{(n-a)^2}, \quad (2)$$

where E_∞ is the ionization potential, R_O is the Rydberg constant for Oxygen, and a is a constant for a given series obtained by fitting this formula to the highest level reported in the NIST database. The resulting atomic model has 84 levels. Note that sublevels belonging to the same term are *not* consolidated into a single level.

Oscillator strengths for all the permitted multiplets in the above O I model were computed by Butler & Zeippen (1991) as part of the Opacity Project and are available in the TOPbase archive. Values for the individual transitions were derived assuming LS-coupling.

Radiative recombination coefficients for the individual triplet terms for a wide range of electron temperatures have been computed by Nahar (1999). Values for the sublevels are derived assuming proportionality to their statistical weights.

Grotrian diagrams for the O I triplet system have been published by Grandi (1975) and Przybilla et al. (2000).

4.2 Recombination cascade

By analogy with the H emission-line spectra of H II regions and planetary nebulae, the most obvious emission mechanism for this O I multiplet is via a radiative cascade following recombinations of O^+ ions to high triplet levels.

Because the ionization potentials of O I (13.618 eV) and H I (13.598 eV) are essentially identical, the emitting volumes for O I and H I recombination lines are also identical, namely the H II region. Accordingly, on the assumption that it is a recombination line, the viability of this identification can be tested by comparing the O I multiplet's emissivity with the estimate given in equation (1).

The emissivity is calculated at $N_e = 4000\text{cm}^{-3}$ and $T_e = 10^4\text{K}$, this being a temperature at which Nahar (1999) tabulates recombination coefficients. The Oxygen abundance is taken to be $n(\text{O})/n(\text{H}) = -3.38\text{dex}$, the B star value adopted by Savage & Sembach (1996).

The calculation proceeds as follows: the rate of recombinations to level i per unit volume is $\alpha_i n(O^+) n_e$, where α_i is the recombination coefficient for level i . These recombinations create a cascade down to the ground term. Accordingly, let \dot{R}_i denote the rate per unit volume at which level i is populated by recombinations directly to i and by cascades from higher levels. Then, since the fraction

$$p_{ij} = A_{ij} / \sum_\ell A_{i\ell} \quad (3)$$

of the population of level i decays to level $j < i$, where A_{ij} is the Einstein A-value for the transition $i \rightarrow j$, the emissivity of this transition is

$$4\pi j_{ij} = p_{ij} \dot{R}_i h\nu_{ij} \quad (4)$$

Moreover, these $i \rightarrow j$ decays make the contribution $p_{ij} \dot{R}_i$ to the quantity \dot{R}_j .

The above calculation is started by setting $\dot{R}_u = \alpha_u n(O^+) n_e$, where u denotes the highest level in the atomic model, and then proceeds downwards level by level to the ground term, resulting in emissivities for all permitted lines in the recombination cascade.

For the three lines contributing to the $4p\ ^3P - 4s\ ^3S^o$ multiplet, the total emissivity is $5.6 \times 10^{-24}\ \text{erg}\ \text{s}^{-1}\ \text{cm}^{-3}$, a mere 0.23 per cent of the required value. But this is a case A calculation in which photons emitted in decays to the ground term escape. For case B, which is obtained by repeating the above calculation with $A_{i\ell} = 0$ for $\ell = 1 - 3$, the emissivity increases to $2.3 \times 10^{-23}\ \text{erg}\ \text{s}^{-1}\ \text{cm}^{-3}$, still only 0.96 per cent of the required value.

4.3 Pumped cascades

If emission in the $4p\ ^3P - 4s\ ^3S^o$ O I multiplet were possible only following recombinations of O^+ ions, then this candidate would now be decisively ruled out. But since the ground term of O I is also a triplet, $\lambda 2.89\mu\text{m}$ emission can also occur via UV pumping of high triplet levels. Accordingly, the suggested emission region is the neutral O zone which, because of the essentially identical ionization potentials noted earlier, is coextensive with the H I region - see Fig. 1. In this region, the far UV but non-ionizing radiation - ie. $\lambda > 911\ \text{\AA}$ - of θ^1 Ori C penetrates and excites O I atoms from the three levels of the ground term to high $^3S^o$ and $^3D^o$ terms, from

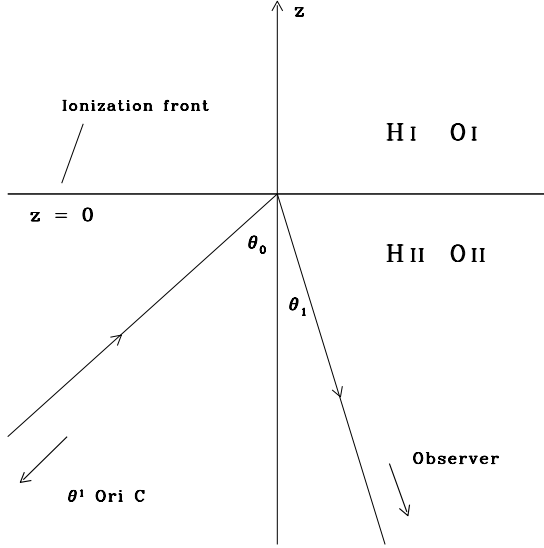


Figure 1. Geometrical configuration assumed for the radiative transfer calculation. Radiation from θ^1 Ori C is incident at angle θ_0 on a semi-infinite uniform layer of neutral Hydrogen and Oxygen. Line emission created in the pumped cascades propagates towards the Observer at angle θ_1 .

whence radiative decays give rise to emission in the λ 2.89 μm multiplet. Exactly the same mechanism was invoked by Grandi (1975) to explain the permitted O I triplet lines in optical spectra of the Orion Nebula.

For this line-formation mechanism, the H II region is not the source of emission; and so the emissivity estimate in equation (1) is no longer the relevant target. Instead, the proposal must be tested by predicting the line's surface brightness. In particular, a viable identification must account for the maximum brightness measured by Rubin et al. (2001),

$$f_{2.89\mu} = 0.12 \text{ bu} \quad , \quad (5)$$

where a brightness unit (bu) of $10^{-13} \text{ erg s}^{-1} \text{ cm}^{-2} \text{ arcsec}^{-2}$ is adopted.

In the remainder of this section, a crude theory is developed with the deliberate aim of overestimating the line's brightness. If this overestimate were to fall short of this maximum, a more detailed treatment would not be necessary.

In computing the line's brightness, we assume that the UV pumping and subsequent de-excitation cascades occur in a semi-infinite uniform slab of neutral O atoms whose surface $z = 0$ is coincident with the Hydrogen ionization front. The incident pumping radiation from θ^1 Ori C has direction cosine $\mu_0 = \cos \theta_0$, and the observer receives radiation emerging at $\mu_1 = \cos \theta_1$.

Let us consider the pumping line at frequency ν_k corresponding to one of the permitted transitions $\ell \rightarrow u$ for $\ell = 1 - 3$ and $u \geq 4$. On the assumption of zero attenuation in the H II region by either dust or neutral O atoms, the intensity at $z = 0$ of the radiation from θ^1 Ori C is $I_k = F(\nu_k)$, where $\pi F(\nu_k)$ is the emergent flux at ν_k from the star's atmosphere. Accordingly, the rate per unit area

at which energy in the frequency interval $(\Delta\nu)_k$ centred on ν_k crosses into the O I zone is

$$\dot{E}_k = I_k \mu_0 (\Delta\nu)_k (\Delta\omega)^* \quad . \quad (6)$$

Here $(\Delta\omega)^* = \pi(R/d)^2$ is the solid angle subtended by θ^1 Ori C from the point considered at the ionization front. Note that the contribution of diffuse radiation from the H II region is neglected.

If we now assume that all the energy in the interval $(\Delta\nu)_k$ is absorbed in the slab by neutral O atoms, then $\dot{E}_k/h\nu_k$ is the rate at which the ν_k line photons excite level u per unit area. Let us further suppose that each of these pumping events leads on average to the emission of $\epsilon_{ij}^k (< 1)$ cascade photons of frequency ν_{ij} . It then follows that

$$4\pi \int_0^\infty j_{\nu_{ij}} dz = \epsilon_{ij}^k \frac{\nu_{ij}}{\nu_k} \dot{E}_k \quad , \quad (7)$$

where $4\pi j_{\nu_{ij}}$ is the emissivity of the line ν_{ij} .

Because the cascade photons of interest are in the IR and are emitted by subordinate lines, we can neglect attenuation as they propagate to the surface of the slab. The transfer equation to be solved is therefore simply

$$\mu \frac{dI_\nu}{dz} = j_{\nu_{ij}} \phi_\nu \quad , \quad (8)$$

where ϕ_ν is the cascade line's normalized emission profile. For a uniform O I slab, this profile is independent of z , and so the emergent intensity is

$$I_\nu(\mu) = \frac{1}{\mu} \phi_\nu \int_0^\infty j_{\nu_{ij}} dz \quad . \quad (9)$$

Now if $\vartheta \times \vartheta$ is the element of sky used to define surface brightness, then, neglecting extinction between the ionization front and the observer, the line brightness at frequency ν is $I_\nu(\mu_1) \vartheta^2$. Accordingly, if we integrate over the line profile, the contribution to the brightness of the cascade line $i \rightarrow j$ from the k th pumping transition is

$$f_{ij}^k = \frac{\vartheta^2}{\mu_1} \int_0^\infty j_{\nu_{ij}} dz \quad . \quad (10)$$

Let us now suppose that isotropic macroturbulence with characteristic velocity v_D is the cause of kinematic broadening in the O I slab and write $(\Delta\nu)_k = w_k \Delta\nu_D$, so that w_k is the dimensionless equivalent bandwidth for absorption by the k th pumping line. Then, using equation (7) to eliminate the emissivity integral and substituting \dot{E}_k from equation (6), we obtain

$$f_{ij}^k = \frac{1}{4} \vartheta^2 \times \frac{\mu_0}{\mu_1} \left(\frac{R}{d}\right)^2 \times \epsilon_{ij}^k w_k \times \frac{\nu_{ij}}{\nu_k} F(\nu_k) \Delta\nu_D \quad . \quad (11)$$

Equation (11) gives the contribution to the strength of the line $i \rightarrow j$ from the cascade driven by the k th pumping transition. For the $\lambda 2.89\mu\text{m}$ multiplet, these pumping transitions comprise all the permitted transitions connecting the three states of the ground term $2p^4 \ ^3P$ to the states belonging to the terms $ns \ ^3S^\circ$ with $n \geq 5$ and to the terms $nd^3 \ ^3D^\circ$ with $n \geq 4$. Summation of equation (11) over these pumping transitions gives the required line strength.

In the absence of predictions for the equivalent bandwidths and for the efficiencies with which cascade photons are emitted, we make the optimistic estimates that, for all k ,

$w_k = 5$ and $\epsilon_{ij}^k = 1$. In addition, we assume blackbody emission by θ^1 Ori C with $T_{eff} = 40000K$, and take $R = 11.1R_\odot$ (Lucy 1995).

Because Rubin et al. (2001) observed maximum line brightness at position 1SW, a line-of-sight that passes θ^1 Ori C with a small impact parameter of $\simeq 0.08pc$, we set $d = 0.2pc$, which is Wen & O'Dell's (1995) estimate of this star's distance above the ionization front. In addition, since the line-of-sight with zero impact parameter has $\mu_0 = \mu_1$, we take the orientation factor $\mu_0/\mu_1 = 1$.

Finally, the macroturbulent velocity v_D must be estimated. From their UKIRT spectrum, Rubin et al. (2001) measure the resolved FWHM of the $\lambda 2.89\mu m$ line to be 24 km s^{-1} . If the line were single, this would give $v_D = 14.4 \text{ km s}^{-1}$. But allowing for the three unresolved components with relative strengths from Section 5, we obtain $v_D = 12.7 \text{ km s}^{-1}$, a value that will be used throughout this investigation. Of course, the actual broadening may be dominated by a differentially expanding flow, with a much smaller turbulent component. Evidence of non-thermal broadening of other lines in the spectrum of the Orion Nebula are summarized by O'Dell (2001b).

With these choices of the parameters, the predicted line brightness is

$$f_{2.89\mu} = 1.48 \text{ bu} \quad , \quad (12)$$

which is a factor 12.3 greater than the maximum of 0.12 bu observed by Rubin et al (2001). By thus comfortably exceeding observed line strengths, the proposed identification survives this initial test. In fact, in the absence of alternatives, this is already a powerful argument in favour of the O I multiplet.

Note that, according to this crude theory, the brightness is independent of the Oxygen abundance. This arises because of the assumption that all photons within a fixed bandwidth are absorbed by the pumping lines.

5 IMPROVED THEORY

The simple calculation of Sect. 4.3 is consistent with the identification of the $\lambda 2.89\mu m$ line as the O I multiplet $4p^3P - 4s^3S^o$. Now an escape probability treatment is developed to see if this identification remains viable when the optimistic estimates of $w_k = 5$ and $\epsilon_{ij}^k = 1$ are replaced by actual calculations. In addition, if the identification is confirmed, a more realistic theory will be needed to exploit the measured strengths of this and other O I lines formed by the cascade mechanism.

5.1 Incident intensities

In Sect. 4.3, the incident intensity $I_k = B_{\nu_k}(T_{eff})$, with $T_{eff} = 40000K$. But the pumping lines are in the wavelength range 918-979 Å where line blocking by the Lyman series and by metal lines is expected to be strong. Accordingly, the first improvement is to replace the black body approximation by the Kurucz (1979) LTE line-blanketed atmosphere with $T_{eff} = 40000K$, $\log g = 4.5$ and solar metal abundances. This model was previously used to investigate the fluorescent excitation of [N III] and [Fe I] lines in the Orion Nebula (Lucy 1995).

As a result of this change, the incident intensities for lines with $\lambda < 930 \text{ Å}$ are reduced by up to 25 percent while those with longer wavelengths are increased by up to 60 percent. Yet more accurate would be a NLTE model incorporating spherical extension and the stellar wind (Gabler et al. 1989).

5.2 Equivalent bandwidths

The rate per unit area at which the k th pumping line absorbs energy from the incident beam is

$$\dot{E}_k = \int_0^\infty dz \ 4\pi \int \ell_\nu J_\nu d\nu \quad , \quad (13)$$

where ℓ_ν is the line's absorption coefficient per unit volume and J_ν is the beam's mean intensity at depth z .

On the assumption that the pumping is confined to a layer whose thickness is small compared to the distance d of θ^1 Ori C, $J_\nu = I_\nu \times (\Delta\omega)^*/4\pi$, where I_ν , the beam's specific intensity, is given by

$$I_\nu = I_k \exp[-(k_\nu + \ell_\nu + m_\nu) \frac{z}{\mu_0}] \quad (14)$$

Here k_ν is the absorption coefficient of unit slab volume due to interstellar grains and m_ν is the summed absorption coefficients of any other pumping lines that overlap the line considered, and which therefore compete for photons.

If we substitute for J_ν in equation (13) and integrate, we recover equation (6) except that $(\Delta\nu)_k$ is now replaced by $w_k \Delta\nu_D$, with equivalent bandwidth w_k given by

$$w_k = \frac{1}{\Delta\nu_D} \int \frac{\ell_\nu}{k_\nu + \ell_\nu + m_\nu} d\nu \quad . \quad (15)$$

5.2.1 Dust absorption

The extinction coefficient for a typical mixture of interstellar grains can be derived from standard fits to observational data as follows: a line of length s in the O I slab corresponds to optical depth $\tau_\lambda = k_\lambda^{ext} s = 0.4\ell n 10 \times A(\lambda)$, where $A(\lambda)$ is the extinction at λ in magnitudes. This can be expressed in terms of the colour excess $E(B - V)$ by writing $A(\lambda) = A(\lambda)/A(V) \times R_V \times E(B - V)$, where $R_V = A(V)/E(B - V)$ is the ratio of visual to selective extinction. But the colour excess is found to be proportional to the H column density. Thus, we also have $N(H) = n(H)s = \gamma E(B - V)$, with $\gamma \simeq 5.8 \times 10^{21} \text{ atoms cm}^{-2} \text{ mag}^{-1}$ (Bohlin, Savage & Drake 1978). Eliminating s from these formulae, we find that

$$k_\lambda^{ext} = 0.4\ell n 10 \times \frac{A(\lambda)}{A(V)} \times R_V \times \frac{n(H)}{\gamma} \quad , \quad (16)$$

This is evaluated using the equation $A(\lambda)/A(V) = a(x) + b(x)/R_V$, where x is the reciprocal wavelength in μm^{-1} and the functions a and b are the fits to observational data given by Cardelli, Clayton & Mathis (1989). Note that since the pumping lines are such that $10.2 < x < 10.9$, this application implies a modest extrapolation beyond the observed extinction data. The ratio R_V is set = 3.1, the standard value for the diffuse interstellar medium (eg, Cardelli et al. 1989).

Equation (16) gives the sum of the dust absorption and the scattering coefficients. If ϖ_λ is the albedo at λ , the absorption coefficient is

$$k_\lambda = (1 - \varpi_\lambda)k_\lambda^{\text{ext}} . \quad (17)$$

In this investigation, we set $\varpi_\lambda = 0.4$ for all the far-UV pumping lines. This value is suggested by Fig. 8 in Gordon et al. (1994), which summarizes the work of these and earlier workers.

5.2.2 Line absorption

On the assumption that isotropic macroturbulence with characteristic velocity v_D is the dominant broadening mechanism, the normalized line absorption profile is

$$\phi_\nu = \frac{1}{\sqrt{\pi}} \frac{1}{\Delta\nu_D} \exp[-(\frac{\nu - \nu_k}{\Delta\nu_D})^2] , \quad (18)$$

where $\Delta\nu_D/\nu_k = v_D/c$. The resulting line absorption coefficient per unit volume is

$$\ell_\nu = \frac{\pi e^2}{m_e c^2} f_{\ell u} \times \frac{n_\ell}{n(O)} \times n(O) \times \phi_\nu . \quad (19)$$

Here the index $\ell = 1 - 3$ refers to the three levels of the ground term, and the index u refers to the pumped levels belonging to the series $ns\ ^3S^o$ and $nd\ ^3D^o$.

5.2.3 Computed bandwidths

Before calculating the quantities w_k from equation (15), line overlaps must be identified. No overlaps occur for the multiplets $2p^4\ ^3P \rightarrow ns\ ^3S^o$ because the lower levels are well separated and the upper levels are single. But for the multiplets $2p^4\ ^3P \rightarrow nd\ ^3D^o$ overlaps do occur because of the small fine structure splittings of the upper terms. Specifically, the three components $2p^4\ ^3P_2 \rightarrow nd\ ^3D_{1,2,3}^o$ compete for photons, as do the two components $2p^4\ ^3P_1 \rightarrow nd\ ^3D_{1,2}^o$.

In contrast to the calculation of Sect. 4.3, which was independent of the Oxygen abundance, this improved theory depends on $n(O)/n(H)$ through the ratios ℓ_ν/k_ν and m_ν/k_ν . As in Section 4.2, we take $n(O)/n(H) = -3.38$ dex.

In addition, the populations of the levels comprising the ground term must be specified. Assuming proportionality to statistical weights, we set $n_\ell/n(O) = (2J + 1)/9$. In fact, these values are in fair accord with the detailed calculations of Pequignot (1990) for the expected conditions immediately behind the ionization front - i.e., $n(H) \gtrsim 10^5\ \text{cm}^{-3}$, $T \gtrsim 5000\ \text{K}$, $n_e/n(H) \lesssim 0.01$.

The equivalent bandwidths w_k obtained from equation (15) for all relevant pumping lines are plotted in Fig. 2. These widths are all less than the optimistic estimate of 5 used in Sect.4.3. Nevertheless, a substantial number of lines have $w_k \gtrsim 2$, thus indicating effective pumping.

The general trends shown in Fig. 2 are readily understood. Each $^3S^o$ term contributes three lines and their w_k values fall with increasing n due to declining gf -values, which imply greater losses to dust absorption. For the six lines from each $^3D^o$ term, there is the additional effect of line overlap. As a result, overlapped lines with small gf -values are starved of photons and thus make little contribution to the pumping. This effect explains why, for each n , three of the $n\ ^3D^o$ components have $w_k \lesssim 1.3$.

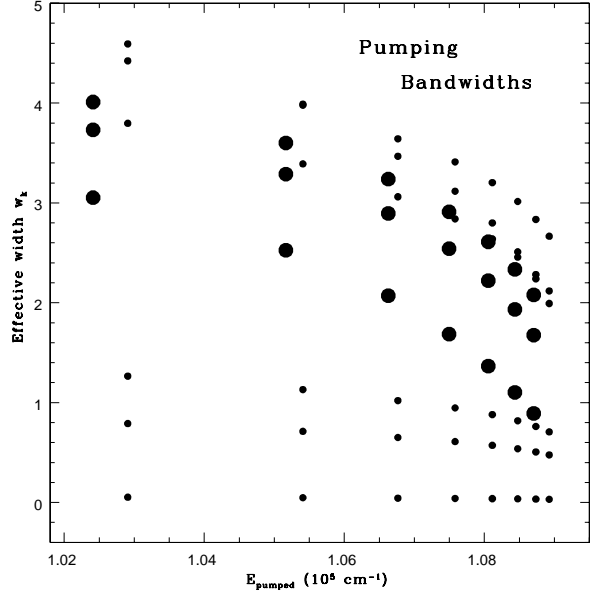


Figure 2. Equivalent bandwidths w_k from equation (15) plotted against the excitation energy of the pumped level. Results are shown for all the pumping transitions contributing to emission in the $O\text{I}\ \lambda 2.89\ \mu\text{m}$ multiplet. Large filled circles identify transitions whose upper levels are $n\ ^3S_1^o$ for $n = 5 - 11$. Small filled circles identify transitions whose upper levels are $n\ ^3D_{1,2,3}^o$ for $n = 4 - 11$.

5.3 Escape probabilities

In cascade calculations, one of two extreme cases is usually considered: case A, in which photons emitted in decays to the ground term escape the nebula; or case B, in which all such photons are re-absorbed by the emitting transitions. In contrast, here we use escape probabilities to treat intermediate circumstances.

For subordinate transitions - i.e. $u \rightarrow \ell$ for $\ell > 3$, the probability of re-absorption is negligible, and so we take their escape probabilities $\beta_{u\ell} = 1$. But for decays to the ground term $2p^4\ ^3P$, the possibility of re-absorption needs to be considered. If a photon of frequency ν is emitted in the decay to level $2p^4\ ^3P_J$, the probability of it being absorbed by a dust grain is $k_\nu/(k_\nu + \ell_\nu + m_\nu)$, where the notation is that of Section 5.2. Thus, by averaging over the line's emission profile, we find that the escape probability is

$$\beta_{u\ell} = \int \frac{k_\nu}{k_\nu + \ell_\nu + m_\nu} \phi_\nu d\nu \quad (20)$$

for $\ell = 1 - 3$ and $u \geq 4$.

If a photon emitted in a decay to the ground term is not absorbed by a dust grain, it is here assumed to be re-absorbed by the emitting transition. But this neglects two effects. First, there is the additional possibility of escaping by crossing back into the H II region - i.e. $z < 0$ in Fig. 1. Second, there is the possibility - for decays from the $^3D^o$ terms - of being absorbed by an overlapping component, thus transferring excitation to a different sublevel of the same $^3D^o$ term.

The first possibility is neglected to avoid a z -dependent cascade calculation, a complexity not warranted at this point. The second possibility is neglected since excitation is

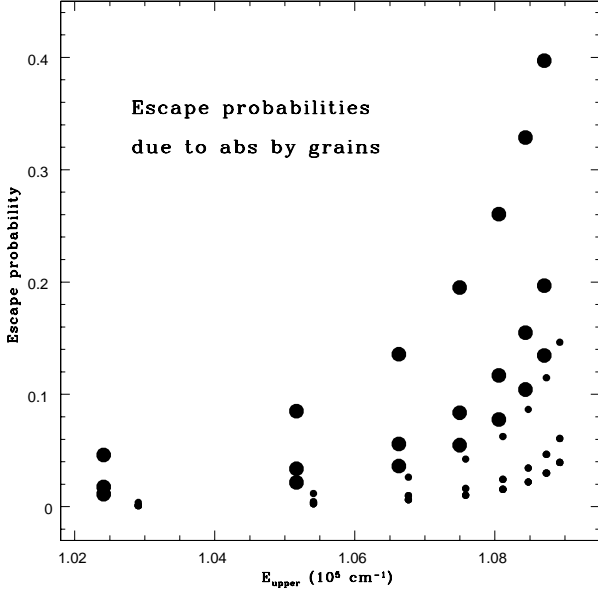


Figure 3. Escape probabilities $\beta_{u\ell}$ from equation (20) plotted against the excitation energy of the emitting level. Large filled circles identify transitions whose upper levels are $n^3S_1^o$ for $n = 5 - 11$. Small filled circles identify transitions whose upper levels are $n^3D_{1,2,3}^o$ for $n = 4 - 11$. Line absorption coefficients are computed on the assumption of Doppler broadening by thermal motions at $T = 10^4 K$.

not lost, merely transferred. As such, this assumption should have little effect on predicted line strengths. (In fact, a code incorporating this interlocking effect has been written, and this statement is confirmed.)

In computing escape probabilities with equation (20), k_ν is calculated exactly as in Section 5.2.1. But the calculation of the line absorption coefficients ℓ_ν and m_ν and the emission profile ϕ_ν departs slightly from Section 5.2.2 in that the macroturbulent velocity v_D is replaced by $\sqrt{2kT/m_O}$, the thermal velocity of the Oxygen atoms. This allows for the possibility that the length scale on which photon recapture occurs is less than that of the bulk motions that determine the broadening of the $\lambda 2.89\mu m$ line. The temperature immediately behind the ionization front is taken to be $T = 10000 K$ (Esteban, Peimbert & Torres-Peimbert 1999).

The resulting escape probabilities are plotted in Fig.3. As for Fig.2, the general trends are readily understood as being due to decreasing gf -values as one ascends the two series. But one point of difference is that the $^3D^o$ terms provide three points on Fig.3 as against six on Fig.2. This is because the quantity $\ell_\nu + m_\nu$ in equation (20) is identical for the three overlapping lines $nd^3D_{1,2,3}^o \rightarrow 2p^4^3P_2$, which therefore have identical escape probabilities. Similarly, the two overlapping lines $nd^3D_{1,2}^o \rightarrow 2p^4^3P_1$ also have identical escape probabilities.

5.4 Efficiencies

With escape probabilities determined, the efficiencies ϵ_{ij}^k can now be derived from the cascade driven by the k th pumping transition. The calculation of the pumped cascades follows closely that for recombinations described in Section 4.2.

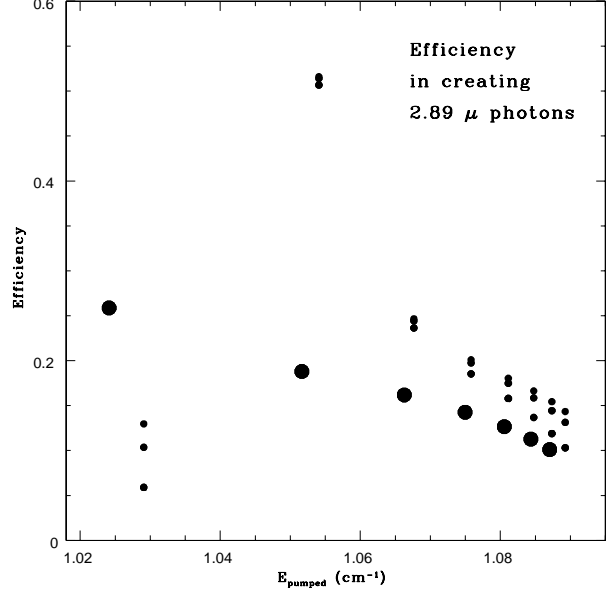


Figure 4. Efficiencies $\epsilon_{2.89\mu}^k$ from equation (22) plotted against the excitation energy of the pumped level. Large filled circles identify transitions whose upper levels are $n^3S_1^o$ for $n = 5 - 11$. Small filled circles identify transitions whose upper levels are $n^3D_{1,2,3}^o$ for $n = 4 - 11$.

The photon absorption rate per unit slab area in the k th pumping line is $\dot{E}_k/h\nu_k$. The quantity \dot{E}_k is derived from equation (6) with $\mu_0 = 1$ and $(\Delta\nu)_k = w_k\Delta\nu_D$, with equivalent bandwidths from Section 5.2.

If the k th pumping line corresponds to the transition $\ell \rightarrow u$, then the k th cascade starts at level u with $\dot{R}_u = \dot{E}_k/h\nu_k$. From a level $i \leq u$, the fraction of decays that go to level j is

$$p_{ij} = A_{ij}\beta_{ij} / \sum_{\ell} A_{i\ell}\beta_{i\ell} \quad , \quad (21)$$

where the escape probabilities are from Section 5.3; and these decays make the contribution $p_{ij}\dot{R}_i$ to \dot{R}_j . As in Section 4.2, this calculation proceeds downwards level by level until the ground term is reached.

When the cascade terminates, photon emission rates $p_{ij}\dot{R}_i$ are available for all permitted cascade transitions $i \rightarrow j$. But these rates were achieved by absorbing pumping photons at the rate $\dot{R}_k = \dot{E}_k/h\nu_k$. Accordingly, the efficiency with which the k th pumping line creates $i \rightarrow j$ photons is

$$\epsilon_{ij}^k = p_{ij}\dot{R}_i / \dot{R}_k \quad . \quad (22)$$

Note that because of the cascade's linearity the efficiencies ϵ_{ij}^k are independent of μ_0 .

The efficiencies with which the numerous pumping lines create $\lambda 2.89\mu m$ photons are plotted in Fig.4. The highest efficiencies of $\simeq 0.51$ are found for the six components of the multiplet $2p^4^3P \rightarrow 5d^3D^o$. But most are in the range 0.1-0.2, a substantial reduction from the optimistic estimate of $\epsilon_{2.89\mu}^k = 1$ used in Section 4.3.

Surprisingly low efficiencies are found for the components of the multiplet $2p^4^3P \rightarrow 4d^3D^o$, with values in the range 0.06-0.13. Inspection of the branching ratios for decay

channels from the $4\ ^3D^\circ$ levels shows that, despite the small escape probabilities for decays to the ground term - see Fig.3 - these still dominate, accounting for 55-80 per cent of the total decay rates from these levels.

The efficiencies plotted in Fig.3 are not an immediately reliable guide to the relative importance of the numerous pumping transitions since a line of high efficiency might have a low equivalent bandwidth. Accordingly, the contribution of each pumped term to the emission of $\lambda 2.89\mu\text{m}$ photons has also been determined. With their percentage contributions in parentheses, the most important terms are: $5\ ^3D^\circ$ (29.4), $5\ ^3S^\circ$ (13.7), $6\ ^3D^\circ$ (10.6), $6\ ^3S^\circ$ (7.7), $4\ ^3D^\circ$ (6.9), and $7\ ^3D^\circ$ (6.4)

5.5 Predicted intensities

With the quantities w_k and ϵ_{ij}^k now calculated, surface brightnesses for all multiplets formed in the cascades are obtained by summing equation (11) over the pumping transitions and over the multiplets' components. The results for all multiplets with $f_\lambda > 0.008$ bu are given in Tables 1 and 2. Table 1 lists the optical lines, with wavelengths in air given in Å. Table 2 lists the infrared lines, with vacuum wavelengths given in μm . The tabulated wavelengths λ_{eff} are the multiplets' effective wavelengths, computed by weighting each component's λ by that component's fractional contribution to f_λ .

The cascades also result in a UV line spectrum extending almost to the Lyman limit. These are not tabulated but we note that the two strongest UV lines are the $3s\ ^3S^\circ - 2p^4\ ^3P$ multiplet at $\lambda 1304.28\text{Å}$ and the $4d\ ^3D^\circ - 2p^4\ ^3P$ multiplet at $\lambda 973.02\text{Å}$. The predicted strengths of these lines are 16.7 and 2.11 bu, respectively.

Of most immediate interest is the predicted strength for the $4p\ ^3P - 4s\ ^3S^\circ$ O I multiplet at $\lambda 2.89\mu\text{m}$. From Table 2, we find that

$$f_{2.89\mu} = 0.14\ \text{bu} \quad , \quad (23)$$

remarkably close to the maximum value of 0.12 bu measured by Rubin et al. (2001) at position 1SW. Since the geometrical parameters $d = 0.2\text{pc}$ and $\mu_0/\mu_1 = 1$ were chosen to represent this point, this outcome is compelling evidence in favour of the proposed identification.

6 DISCUSSION

In this section, further testing of the proposed identification is carried out using the theoretical understanding developed in Section 5. In addition, the sensitivity of the results to various input parameters is briefly discussed.

6.1 Theory-independent estimates

Because the prediction of about the right strength for the O I multiplet at $\lambda 2.89\mu\text{m}$ has required a rather complicated, multi-parameter theory, it is of interest that this multiplet's strength can be reliably estimated without invoking this theory. There are two ways of doing this, both of which are independent of the line formation mechanism and of the distribution of O I along the line-of-sight.

The first estimate follows from noting that the proposed

identification has the same upper term ($4\ ^3P$) as the O I line at $\lambda 4368\text{Å}$. Accordingly, whenever the 4368Å line is observed, we can confidently infer that emission at $\lambda 2.89\mu\text{m}$ is also occurring and can compute the IR multiplet's strength from the formula $f_{2.89\mu} = f_{0.44\mu}/1.48$ - see Tables 1 and 2. This calculation depends only on the A-values and frequencies of the transitions.

For a definitive test of the O I identification using this accurately known intensity ratio, the measured optical and IR line strengths are needed at exactly the same location. Unfortunately, this information seems not to be available from published spectra. Failing this, the approach adopted here is to use the measured strengths of the $\lambda 4368\text{Å}$ line at locations near to 1SW to infer strengths for the $\lambda 2.89\mu\text{m}$ line. This can be done using the data of Esteban et al. (1998).

Esteban et al. (1998) report that the $\lambda 4368\text{Å}$ multiplet has reddening-corrected brightnesses of 0.036 and 0.060 bu at their slit positions 1 and 2. The inferred values for the $\lambda 2.89\mu\text{m}$ line are therefore 0.024 and 0.040 bu, both of which represent averages over the $13.3'' \times 2''$ slit and refer to positions offset from θ^1 Ori C by 45 and 27'', respectively.

These inferred values are significantly less than the maximum of 0.12 bu observed by Rubin et al (2001) at 1SW, a position offset from θ^1 Ori C by 32''. But this latter measurement refers to a $0.74\ \text{arcsec}^2$ aperture extracted from their long-slit UKIRT spectrum. On the other hand, from their ISO SWS02 spectrum with a $14'' \times 20''$ aperture also centered on 1SW, they report an average brightness for the $\lambda 2.89\mu\text{m}$ line of 0.039 bu. This is in satisfactory agreement with the spatial averages inferred from the data of Esteban et al. (1998) at similar offsets from the UV source. Accordingly, these theory-independent estimates strongly support the identification of the $\lambda 2.89\mu\text{m}$ line as the $4p\ ^3P - 4s\ ^3S^\circ$ multiplet of O I.

The second theory-independent estimate derives from noting that other observed optical O I lines tell us that terms higher than $4\ ^3P$ also emit. Accordingly, if the cascade from such a term results in the emission of the $\lambda 2.89\mu\text{m}$ multiplet, this emission's intensity ratio to the observed optical line can be computed; and this allows a *contribution* to the strength of the $\lambda 2.89\mu\text{m}$ line to be estimated from the strength of the optical line. Note, however, that, when the excited upper term is $^3D^\circ$, the intensity ratios depend on the relative populations of the $^3D^\circ$ term's sublevels. Also the cascades overlap so the contributions to the $\lambda 2.89\mu\text{m}$ line cannot simply be co-added. Partly because of these complications, this means of estimating the strength of the $\lambda 2.89\mu\text{m}$ is not pursued further. But the main reason is that it is more rewarding to use the information in the other optical O I lines to test the cascade theory of Section 5.

These two theory-independent procedures can of course be applied to infer the presence of and to estimate strengths for numerous other O I lines in the IR. Since the observed optical lines at $\lambda 5275$ and 5299Å imply excitation of levels as high as $7\ ^3D^\circ$ and $8\ ^3S^\circ$, most of the IR lines in Table 2 must be present at some level at Positions 1 and 2 of Esteban et al. (1998). But again, rather than proceed with such estimates, it is preferable to use the data to test the cascade theory. If the test is successful, *ratios* of line strengths from Tables 1 and 2 should be reliable and so can be used to estimate strengths of IR lines from observed optical lines.

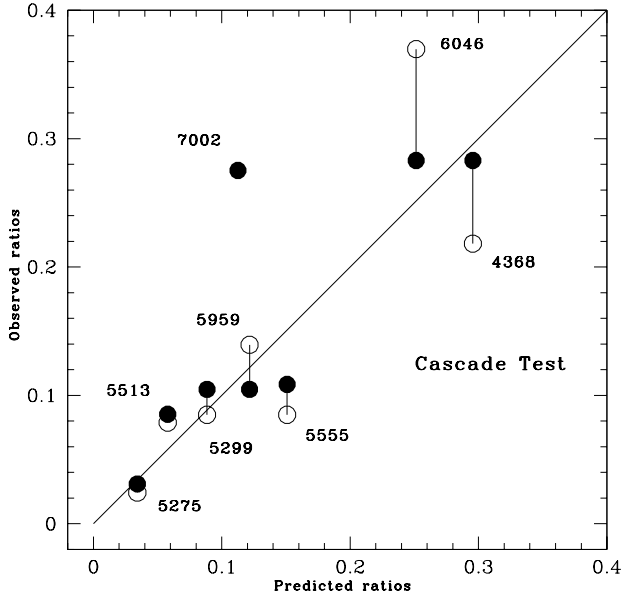


Figure 5. Cascade test for permitted O I emission lines in the optical spectrum of the Orion Nebula. Open and filled circles refer to Positions 1 and 2, respectively, of Esteban et al. (1998) and correspond to the indicated wavelength in Å. The theoretical values are from Table 1.

6.2 Cascade test

As noted earlier, Grandi (1975) has previously demonstrated convincingly that pumped cascades account for the permitted O I triplet lines in optical spectra of the Orion Nebula. Nevertheless, it is of interest to test the cascade hypothesis again using the theoretical treatment given here together with the modern CCD measurements of Esteban et al. (1998).

The results of the cascade test are shown in Fig.5 where both the observed and predicted line brightnesses are expressed as fractions of the summed values for the lines $\lambda\lambda 4368, 5275, 5299, 5513, 5555, 5959$ and 6046Å . (The line $\lambda 7002\text{Å}$ is excluded from this sum because it was observed only at Position 2.) Inspection of Fig. 5 reveals a satisfactory degree of agreement between theory and observation for all but one of the eight observed lines. The exception is the line at $\lambda 7002\text{Å}$.

A point to note in assessing the success of this test is the complexity of this cascade mechanism when compared to a simple recombination cascade. In this case, predicted line strengths represent the superposition of numerous separate pumped cascades whose relative importance is determined by dust absorption through its effect on equivalent bandwidths and escape probabilities. Evidently, there are interesting diagnostic possibilities to be exploited using accurate measurements of the strengths of these and other optical O I lines.

Note that none of the observed optical lines has a strength that can be computed via a simple cascade calculation from one of the other optical lines. Thus Fig.5 is free from this species of degeneracy, which further emphasizes its diagnostic importance.

6.3 Wavelength

To be accepted, a line identification must be consistent with the measured wavelength of the uid line. From their ISO SWS02 spectrum, Rubin et al. (2001) infer a rest wavelength of $2.89350 \pm 0.00003\mu\text{m}$, in essentially perfect agreement with $\lambda_{eff} = 2.893509\mu\text{m}$ from Table 2.

However, Rubin et al. derived this wavelength assuming that line formation occurs in the main H II region at $V_{helio} = 17 \text{ km s}^{-1}$. But for the proposed identification, line formation occurs immediately behind the ionization front, for which an appropriate velocity is 25.5 km s^{-1} (O'Dell 2001a). Thus there is in fact a wavelength discrepancy equivalent to $8\text{-}9 \text{ km s}^{-1}$, significantly larger than the Rubin et al. error estimate of 3 km s^{-1} . But given that a theory-independent argument (Section 6.1) places an O I line with about the right strength at this slight velocity offset, this discrepancy is not grounds for discarding the identification.

A possible explanation of this velocity offset is that that the UV pumping occurs predominantly in neutral blobs entrained in the outflowing ionized gas.

6.4 Intensity profile

Rubin et al. (2001) found that the highest surface brightness for the uid line is coincident with the brightest part of the H II region, and therefore understandably concluded that it originates from within the main ionization zone. But the O I $\lambda 2.89\mu\text{m}$ identification conflicts with this conclusion; and so there is the obvious expectation that it will fail to yield a satisfactory distribution of surface brightness.

A crude calculation of the angular distribution of O I cascade emission can be made using the 3-D model of the Orion Nebula constructed by Wen & O'Dell (1995). Fig.5 of their paper gives the cross section at position angle 226° , which includes the brightest part of the Nebula. To a sufficient approximation, their profile for the ionization front can be modelled as three straight line segments. Taking 500 pc as the distance of the Nebula, we can use this model to compute the distance d in pc from θ^1 Ori C to a point on the ionization front. The direction cosines μ_0 and μ_1 - see Fig.1 - at this point can also be computed if we add the assumption that the ionization front is not tilted in the direction perpendicular to this cross section. In this way, the geometrical factor

$$C = \frac{\mu_0}{\mu_1} \left(\frac{0.2}{d} \right)^2, \quad (24)$$

can be derived and used to obtain the intensity profiles of the O I cascade lines from the reference line brightnesses given in Tables 1 and 2.

In Fig.6, the resulting intensity profile for the O I $\lambda 2.89\mu\text{m}$ multiplet is plotted for position angle 226° . This should be compared to Fig. 5a in Wen & O'Dell (1995), which plots intensity profiles for [N II], H α and [O III] lines at this same position angle. This comparison shows that O I line has a predicted intensity profile that is qualitatively similar to those of lines emitted by the H II region. In particular, peak intensities at offsets of $\simeq 30''$ to the SW are closely coincident, and all profiles show a similar steep decline beyond their peaks in the SW. Thus the observed intensity profile of the uid line, though suggestive of emission from within

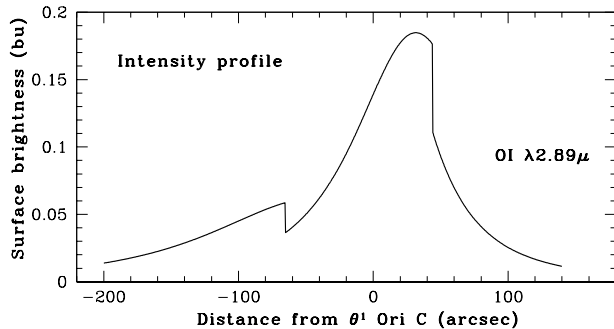


Figure 6. Intensity profile for O I $\lambda 2.89\mu\text{m}$ emission. This 1-D profile is at position angle 226° and corresponds to Fig. 5 in Wen & O’Dell (1995).

the H II region, is in fact also consistent with line formation by pumped cascades in the neutral zone immediately behind the ionization front.

Note that the discontinuities in Fig.6 at offsets of -65 and $+45''$ are due to the discontinuities of μ_0/μ_1 at points where the linear segments meet.

6.5 Sensitivity

In this subsection, the sensitivity of the cascade calculation to input parameters is investigated. Given the strong evidence already presented in support of the O I identification, the main interest now is the possible relevance of this line and, more importantly, of the optical lines for diagnostic investigations.

6.5.1 Oxygen abundance

An increase of $n(\text{O})/n(\text{H})$ by 0.1dex increases the strength of the $\lambda 2.89\mu\text{m}$ multiplet by 0.032dex, thus confirming the insensitivity to abundance anticipated by the crude theory of Section 4.

With respect to the observed optical lines, the responses to this change range from 0.013dex ($\lambda 5959\text{\AA}$) to 0.067dex ($\lambda 7002\text{\AA}$). This illustrates a useful differential sensitivity that can perhaps be exploited diagnostically.

6.5.2 Gas-to-dust ratio

The number density of grains in the O I slab is determined by the coefficient γ in the empirical formula of Bohlin et al. (1978) - see Section 5.2.1. Decreasing this number density by 1.0dex by increasing γ to $5.8 \times 10^{22} \text{ atoms cm}^{-2} \text{ mag}^{-1}$ results in a 0.23dex increase in the $\lambda 2.89\mu\text{m}$ line. The corresponding changes in the optical lines range from 0.10dex ($\lambda 5959\text{\AA}$) to 0.46dex ($\lambda 7002\text{\AA}$).

6.5.3 Ratio of visual to selective extinction

The dust absorption coefficient calculated in Section 5.2.1 assumes $R_V = 3.1$. This ratio is known to depend on environment, with $R_V = 5$ found in some dense clouds (e.g., Cardelli et al. 1989). With this value, the strength of the $\lambda 2.89\mu\text{m}$ line increases by 0.044dex. The corresponding changes in

the optical lines range from 0.018dex ($\lambda 5959\text{\AA}$) to 0.091dex ($\lambda 7002\text{\AA}$).

6.5.4 Microturbulence

The adopted kinematic model with $v_D = 12.7 \text{ km s}^{-1}$ has been described as *macroturbulence* because it does *not* apply on the shortest length scales, namely the mean free paths of photons emitted in decays to the O I ground term. On these scales, thermal broadening has been assumed. If this assumption is dropped, and the Doppler parameter in Section 5.3 also set $= 12.7 \text{ km s}^{-1}$, then the kinematic model becomes one of *microturbulence*.

With this change, the strength of the $\lambda 2.89\mu\text{m}$ line changes by -0.058dex . The corresponding changes in the optical lines range from $+0.001\text{dex}$ ($\lambda 5959\text{\AA}$) to -0.30dex ($\lambda 7002\text{\AA}$). Notice that this change would seriously worsen the already substantial discrepancy for the $\lambda 7002\text{\AA}$ line in Fig.5.

6.5.5 Temperature of O I slab

In the calculation of escape probabilities (Section 5.3), thermal broadening is assumed at $T = 10000\text{K}$. If this temperature is reduced to 3000K , the $\lambda 2.89\mu\text{m}$ line’s strength increases by 0.035dex. The corresponding changes in the optical lines range from 0.005dex ($\lambda 5959\text{\AA}$) to 0.14dex ($\lambda 7002\text{\AA}$).

7 CONCLUSION

The aim of this investigation has been to identify the strong $\lambda 2.89\mu\text{m}$ emission line discovered by Rubin et al. (2001). Surprisingly, the identification turns out to be a line from a neutral atom (O I) rather than from an ion with a production ionization potential between 13.6 and 54.4 eV as expected by Rubin et al. Correspondingly, the line originates not from within the H II region but from the neutral zone behind the ionization front. Because the Orion Nebula is a *thin* blister of ionized gas on the near side of the Orion Molecular Cloud (eg, O’Dell 2001b), lines-of-sight through the densest part of the H II region also intersect the ionization front and therefore also the neutral zone where UV pumping of O I occurs. This explains why an O I cascade line can have a spatial intensity profile that mimics those of emission lines originating in the H II region (Section 6.4).

On a memorable previous occasion, puzzling uid nebular emission lines also proved to be due to Oxygen (Bowen 1927), with momentous consequences for astronomical spectroscopy (eg, Osterbrock 1988). In the present case, by contrast, one could argue that the identification is almost totally inconsequential given that that the strength of the $\lambda 2.89\mu\text{m}$ line can be inferred from that of the $\lambda 4368\text{\AA}$ line (Section 6.1). However, the treatment of O I cascades stimulated by this uid line reveals interesting diagnostic possibilities, most or even all of which can be exploited with measurements of the optical O I lines. First, the cascades occur within a very narrow zone immediately behind the ionization front. For example, with $n(\text{H}) = 10^5 \text{ cm}^{-3}$ and $v_D = 12.7 \text{ km s}^{-1}$, the length scale corresponding to $\tau = 1$ at the line centre of the third strongest line pumping the 5^3D^o term is $4 \times 10^{-5} \text{ pc}$, equivalent to an angular scale of about $0.02''$. Thus

Table 1. Optical O I lines formed in pumped cascades

λ_{eff}	Multiplet	f_λ (bu)
3433.43	$6p\ ^3P - 3s\ ^3S^o$	0.0083
3692.38	$5p\ ^3P - 3s\ ^3S^o$	0.0427
4368.24	$4p\ ^3P - 3s\ ^3S^o$	0.2074
4925.65	$11d\ ^3D^o - 3p\ ^3P$	0.0080
4972.47	$10d\ ^3D^o - 3p\ ^3P$	0.0098
4980.05	$11s\ ^3S^o - 3p\ ^3P$	0.0175
5037.46	$9d\ ^3D^o - 3p\ ^3P$	0.0125
5047.74	$10s\ ^3S^o - 3p\ ^3P$	0.0259
5131.24	$8d\ ^3D^o - 3p\ ^3P$	0.0166
5146.57	$9s\ ^3S^o - 3p\ ^3P$	0.0391
5275.07	$7d\ ^3D^o - 3p\ ^3P$	0.0240
5299.00	$8s\ ^3S^o - 3p\ ^3P$	0.0621
5512.71	$6d\ ^3D^o - 3p\ ^3P$	0.0406
5554.95	$7s\ ^3S^o - 3p\ ^3P$	0.1059
5958.52	$5d\ ^3D^o - 3p\ ^3P$	0.0854
6046.38	$6s\ ^3S^o - 3p\ ^3P$	0.1764
7002.12	$4d\ ^3D^o - 3p\ ^3P$	0.0790
7254.36	$5s\ ^3S^o - 3p\ ^3P$	0.3007
8446.48	$3p\ ^3P - 3s\ ^3S^o$	2.1353
9723.43	$8p\ ^3P - 3d\ ^3D^o$	0.0094

velocity measurements of the permitted O I lines potentially give a sharply defined reference velocity for studies of the dynamics of the Orion Nebula. There is also the possibility of investigating the clumpiness of O I and therefore H I at the point of photoionization by θ^1 Ori C (Section 6.3). In view of the abundance of Oxygen and the high gf -values of the pumping transitions, this superb resolution in depth at ionization fronts may never be surpassed.

The second point concerning diagnostic potential is that intensity ratios of optical lines are *not* simply derivable from A-values and frequencies (Section 6.2): the astrophysics determining the relative importance of the numerous independent cascades needs also to be correct; and this leads to these lines having usefully different sensitivities to input parameters (Section 6.5).

Yet another possibility is to exploit the geometrical factor C - equation (24) - to determine the topography of the Orion Nebula's ionization front independently of the procedure followed by Wen & O'Dell (1995). However, in such an investigation, it may be preferable to replace the orientation factor μ_0/μ_1 by an average derived from a statistical model of clumpiness.

These intriguing diagnostic possibilities have not been pursued in this paper beyond noting that a substantial evacuation of grains from the cascade zone reduces the $\lambda 7002\text{\AA}$ line's discrepancy in Fig.5, and that a *microturbulent* kinematic model would increase this discrepancy.

8 ACKNOWLEDGEMENTS

I am indebted to M.J.Barlow for bringing this problem to my attention. K.Butler, K.A.Berrington, S.N.Nahar and R.H.Rubin kindly provided information and unpublished data. The final form of this paper benefited from stimulating discussions with M.J.Barlow, X.-W.Liu and other members of the nebular astrophysics group at UCL as well as from comments by the referee, C.R.O'Dell.

Table 2. Infrared O I lines formed in pumped cascades

λ_{eff}	Multiplet	f_λ (bu)
1.032313	$6p\ ^3P - 4s\ ^3S^o$	0.0142
1.044628	$7p\ ^3P - 3d\ ^3D^o$	0.0131
1.128987	$3d\ ^3D^o - 3p\ ^3P$	0.4272
1.185827	$8d\ ^3D^o - 4p\ ^3P$	0.0103
1.187145	$6p\ ^3P - 3d\ ^3D^o$	0.0173
1.194037	$9s\ ^3S^o - 4p\ ^3P$	0.0083
1.265549	$7d\ ^3D^o - 4p\ ^3P$	0.0148
1.308046	$5p\ ^3P - 4s\ ^3S^o$	0.0378
1.316817	$4s\ ^3S^o - 3p\ ^3P$	0.5303
1.411486	$6d\ ^3D^o - 4p\ ^3P$	0.0270
1.567012	$5p\ ^3P - 3d\ ^3D^o$	0.0202
1.745830	$5d\ ^3D^o - 4p\ ^3P$	0.1028
1.823426	$6s\ ^3S^o - 4p\ ^3P$	0.0320
2.857113	$6p\ ^3P - 5s\ ^3S^o$	0.0083
2.893509	$4p\ ^3P - 4s\ ^3S^o$	0.1401
3.098498	$4d\ ^3D^o - 4p\ ^3P$	0.0133
3.453334	$6d\ ^3D^o - 5p\ ^3P$	0.0302
3.661737	$5s\ ^3S^o - 4p\ ^3P$	0.0430
4.560809	$4p\ ^3P - 3d\ ^3D^o$	0.0216
5.985350	$7d\ ^3D^o - 6p\ ^3P$	0.0102
6.858507	$5p\ ^3P - 5s\ ^3S^o$	0.0238

REFERENCES

- Berrington K.A., 2001, in preparation
 Bohlin R.C., Savage B.D., Drake J.F., 1978, ApJ 224,132
 Bowen I.S., 1927, PASP, 39,295
 Butler K., Zeippen C.J., 1991, J.Phys. IV, Colloq. C1, 141
 Cardelli J.A., Clayton G.C., Mathis J.S., 1989, ApJ,345,245
 Esteban C., Peimbert M., Torres-Peimbert S., Escalante V. 1998, MNRAS, 295, 401
 Esteban C., Peimbert M., Torres-Peimbert S., 1999, A&A, 342, L37
 Gabler R., Gabler A., Kudritzki R.P., Puls J., Pauldrach A., 1989, A&A, 226,162
 Garstang R.H., 1957, MNRAS, 117, 393
 Gordon K.D., Witt A. N., Carruthers G.R., Christensen S.A., Dohne B.C., 1994, ApJ,432,641
 Grandi S.A., 1975, ApJ, 196, 465
 Kurucz R.L., 1979, ApJS, 40,1
 Kurucz R.L., Bell B., 1995, Kurucz CD-ROM No.23
 Lucy L.B., 1995, A&A, 294,555
 Nahar S.N., 1999, ApJS, 120,131
 O'Dell C.R., 2001a, PASP, 113,29
 O'Dell C.R., 2001b, ARAA, 39,99
 Osterbrock D.E., 1988, PASP, 100,412
 Osterbrock D.E., Tran H.D., Veilleux S., 1992, ApJ, 389,305
 Pequignot D., 1990, A&A, 231, 499
 Przybilla N., Butler K., Becker S.R., Kudritzki R.P., Venn K.A., 2000, A&A, 359,1085
 Rubin R.H., Geballe T.R., Colgan S.W.J., Dufour R.J., 2000,IAUJD1.059P
 Rubin R.H., Dufour R.J., Geballe T.R., Colgan S.W.J., Harrington J.P., Lord S.D, Liao A.L., & Levine D.A. 2001 in Spectroscopic Challenges of Photoionized Plasmas, ASP Conference series, Eds. G.J. Ferland & D.W. Savin 2001 (in press) (astro-ph/0109398)
 Savage B.D., Sembach K.R. 1996, ARAA, 34,279
 Seaton M.J., Yan Y., Mihalas D., Pradhan A.K., 1994, MNRAS, 266, 805
 Storey P.J., Hummer D.G. 1995, MNRAS, 272,41
 Wen Z., O'Dell C.R., 1995, ApJ, 438, 784